Nuclear Instruments and Methods in Physics Research A 637 (2011) S76–S79

Contents lists available at ScienceDirect

Nuclear Instruments and Methods in Physics Research A

journal homepage: www.elsevier.com/locate/nima

Driver linac design for a femtosecond head-on inverse Compton scattering X-ray source

N.Y. Huang [a], W.K. Lau [b,*], C.C. Liang [b], A.P. Lee [b], W.C. Cheng [c], S.S. Yang [a]

[a] Institute of Photonics Technologies, National Tsing Hua University, Hsinchu 30013, Taiwan
[b] National Synchrotron Radiation Research Center, Hsinchu 30076, Taiwan
[c] Institute of Electro-Optical Engineering, National Chiao Tung University, Hsinchu 30010, Taiwan

ARTICLE INFO

Available online 10 February 2010

Keywords:
Femtosecond beam
Inverse Compton scattering

ABSTRACT

The feasibility of generating an ultra-short relativistic electron beam with a thermionic cathode rf gun driver linac for a femtosecond head-on inverse Compton scattering (ICS) X-ray source has been examined by space charge tracking throughout the entire beamline, from the cathode to the interaction point. It has been determined that GHz-repetition-rate electron pulses as short as 49 fs can be produced by compressing the energy-chirped beam from a 2998-MHz, 1.5-cell rf gun with an alpha magnet and an rf linac operating at the injection phase near the zero crossing. These electron pulses, with a 42-pC bunch charge, are accelerated to 27 MeV with an S-band traveling-wave constant-gradient linac structure for the ICS in an interaction chamber located downstream. The driver linac design that allows the operation of an ultra-short ICS X-ray source at a 0.7-Å wavelength, with a peak photon flux of 9.08×10^{17} photons/s, is presented in this paper.

1. Introduction

The high-brilliance femtosecond X-ray source is an indispensable tool for studying ultra-fast structural dynamics. In contrast to a large-scale X-ray free-electron laser (FEL) user facility, such as LCLS at SLAC National Laboratory, the femtosecond ICS X-ray source is much more compact and less expensive to construct. Despite the fact that the ICS X-ray source is weaker than the X-ray FEL in intensity, its peak brilliance is still comparable to a third-generation ring-based synchrotron light source. Furthermore, unlike the X-ray FEL, the moderate photon flux from an ICS source is less damaging to most samples and allows repetitive pump-probe measurements [1]. In this work, we perform space charge tracking of the electron beam, starting from the cathode and to the interaction point in the scattering chamber throughout the whole beamline. We put forth a driver linac design for the generation of an ultra-short relativistic electron beam with a thermionic cathode rf gun and an alpha magnet, which worked as a low-energy bunch compressor [2]. With this linac design, a sub-hundred femtosecond high-peak-brilliance hard X-ray source via head-on ICS has been proposed.

The ICS is the interaction between a relativistic electron bunch and a laser pulse so that the motion of the relativistic electron in the bunch is modulated by the laser field, and the wavelength of the backscattered photon is up-shifted by a factor of γ^2 [3]. The wavelength of the backscattered photon, λ_x, is related to the electron beam energy and the laser wavelength, λ_0, as indicated in Eq. (1), where γ is the Lorentz factor and a_0 is the laser strength parameter, which is related to the laser intensity by $a_0 = 0.85 \times 10^{-9}[\lambda_0(\mu\text{m})][I_0(\text{W/cm}^2)]^{1/2}$:

$$\lambda_X = \lambda_0(1 + a_0^2/2)/4\gamma^2 \quad (1)$$

The head-on ICS is capable of producing more photons per pulse in comparison with the orthogonal scheme, in which the laser interacts with the electron beam at a right angle. However, the pulse duration of the backscattered X-ray from the head-on ICS is limited by the length of the electron bunch, but not by that of the laser pulse. The number of backscattered X-ray photons per pulse for a head-on ICS with a laser and an electron beam can be estimated from Eq. (2) [4]:

$$N_X = \alpha(I_b/e) f \tau_X N_0 a_0^2 \quad (2)$$

where $\alpha = 1/137$ is the fine structure constant; I_b is the electron bunch current; f is the filling factor of the electron beam cross-section by the laser and is equal to one when their focal radii at the interaction point are the same; and τ_X is the X-ray pulse duration, which is the same as the electron bunch length for the head-on ICS. $N_0 = (1 + \overline{\beta}_z)cT/\lambda_0$ is the number of laser periods in which a single electron interacts, where cT is the effective interaction time, and this value is equal to the laser pulse length in our case. It is worth noting that an electron beam with a

* Corresponding author. Tel.: +886 3 5780281; fax: +886 3 5783890.
E-mail address: wklau@nsrrc.org.tw (W.K. Lau).

0168-9002/$ - see front matter © 2010 Elsevier B.V. All rights reserved.
doi:10.1016/j.nima.2010.02.026

smaller beam size and shorter pulse length helps to improve the backscattered photon flux.

This paper is organized as follows. Our experimental setup for the ICS experiment at NSRRC is briefly described in Section 2. The design considerations for this driver linac and femtosecond beam dynamics in the electron beamline are discussed in Section 3. The last section details our conclusion.

2. The NSRRC head-on ICS experiment

In our setup, as shown in Fig. 1, a 2998-MHz flat cathode rf gun that operates at an uneven half-cell to full-cell field ratio is used to produce a linearly energy-chirped beam for bunch compression with an alpha magnet located downstream. The field ratio of the rf gun is set at 1:2 for the initial experiments. A slit (collimator) is installed in the alpha magnet for beam energy selection. An S-band constant-gradient traveling-wave linac is used to accelerate the beam and to freeze the bunch phase at the desired energy. A variable high-power phase shifter is installed to allow linac operation at different injection phases. The 798-nm Ti:sapphire laser used in this experiment is originally used as the drive laser for a photoinjector. The peak power of this laser is 37.5 GW at ~100 fs pulse duration, and it is adequate for the demonstration of an ultra-fast ICS X-ray source. A dedicated laser system with a higher pulse energy can be used if higher X-ray photon flux is needed in the future. The IR laser used in this experiment, as well as the ultra-short electron bunches, will be focused for collision in the interaction chamber.

3. Linac design considerations and simulation results

The thermionic rf gun is operated at an accelerating field gradient of 25 and 50 MV/m in its half-cell and full-cell, respectively. According to a PARMELA study, the rf gun is able to generate a linearly energy-chirped beam with a charge of about 235 pC and a maximum normalized momentum of about 6.0 (Fig. 2). Since the head of a bunch from the thermionic rf gun has higher energy than its tail, the bunch tends to decompress in drift sections. The alpha magnet helps to rotate the particle distribution in the longitudinal phase space clockwise, and the collimator inside the alpha magnet can be used to select the desired range of electron momentum. However, one must over-compress the bunch slightly in the alpha magnet in order to compensate for the bunch lengthening effect in the downstream drift sections. The beam is accelerated to higher energy by the rf linac until all electrons in the bunches move more or less at the same speed. That is, the electron distribution of the compressed bunch in the longitudinal phase space remains unchanged in the drift section after the linac. Two operating conditions of the linac are interesting to this study. The first is when the electron bunch is injected into the booster linac near the rf phase for maximum energy gain. The second is when the bunch is injected near the zero crossing rf phase for additional bunch compression; i.e. velocity bunching [5]. Besides the bunch length compression, the beam must be focused to a tiny spot at the interaction point to obtain a high peak photon flux X-ray by proper tuning of the quadrupole pair. We expected that the beam at the interaction point could be focused to 30 μm.

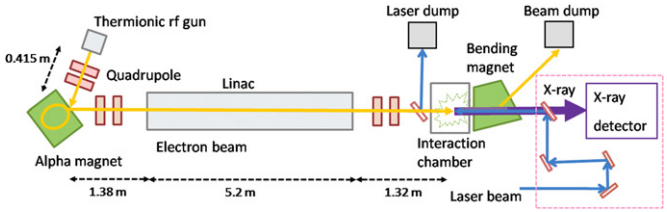

Fig. 1. Setup for the NSRRC head-on ICS experiment.

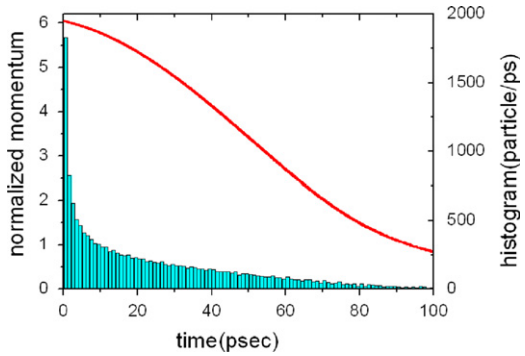

Fig. 2. Electron distribution at the thermionic rf gun exit.

3.1. Parametric study

Optimization of the beamline parameters for the shortest electron bunch is done mainly with ELEGANT [6]. Particle distribution at the gun exit, as calculated by PARMELA [7], is transferred to ELEGANT for particle dynamics calculations at specific beamline element settings. A minimum bunch length of 63.68 fs can be obtained with the alpha magnet gradient operating at 256 Gauss/cm for on-crest operation of the booster linac. In this case, the collimator in the alpha magnet is adjusted to allow only 1.9% of the highest energy particles to pass through, and the electron bunch is accelerated to 24.5 MeV. When the linac is operated at the rf zero crossing, the electron bunch can be compressed to 22.77 fs, with the alpha magnet operating at 460 Gauss/cm. The collimator is adjusted to filter out all electrons except those with energy that fall into the top 2.2% range. Fig. 3 depicts the longitudinal phase space distribution of electrons in the compressed bunch when the linac is operated at the rf crest. Fig. 4 shows the electron distribution in phase space when the linac is operating at the rf zero crossing. The final bunch length can be adjusted by changing the gradient of the alpha magnet and the injection phase of the booster linac under the fixed beamline element settings. Fig. 5 shows the relation between the compressed bunch length and the field gradient of the alpha magnet under the two rf linac injection phases. As seen in Fig. 5, with the booster linac operated at the zero crossing point, the

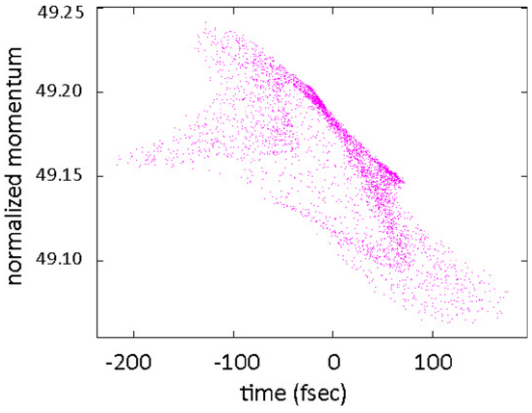

Fig. 3. Electron distribution of the compressed bunch in longitudinal phase space when the linac injection phase is on the rf crest.

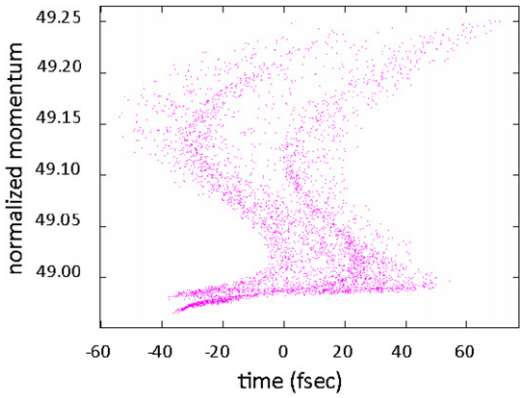

Fig. 4. Electron distribution of the compressed bunch in longitudinal phase space when the linac injection phase is at the rf zero crossing.

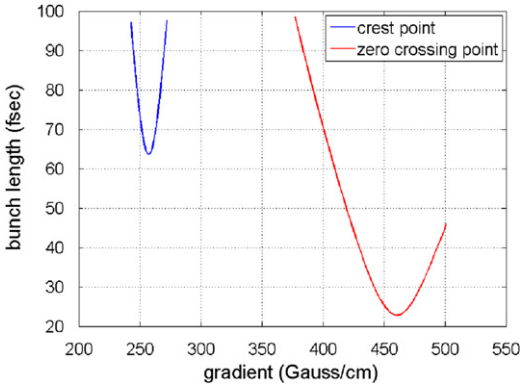

Fig. 5. Bunch length as a function of the alpha magnet gradient when the linac injection phase is on the rf crest (blue) and at the rf zero crossing (red). (For interpretation of the references to colour in this figure legend, the reader is referred to the web version of this article.)

velocity bunching mechanism helps to further compress the electron bunch by a factor of three. However, a larger accelerating gradient is required to keep the beam energy the same after acceleration.

3.2. Space charge effect

Space charge effect is not negligible during bunch compression in our driver linac setup. A general particle tracer (GPT) [8] has been used for simulation of space charge dynamics for the electron beam. Our simulation results show that, without the space charge effect, both ELEGANT and GPT predict similar beam properties. When the space charge effect is considered, with the booster linac phase at zero crossing, the shortest length after bunch compression is about two times larger than the case that does not consider the space charge effect. The evolution of the bunch length, as influenced by the space charge effect, can be seen in Fig. 6. Without the space charge effect, the simulation result is similar to that from ELEGANT. That is, the shortest achievable bunch length is about 22.5 fs. However, with the space charge effect included, the electron bunch length in the linac reaches its minimum at the very beginning of acceleration, and then it decompresses before it gains enough energy from the linac. It has been determined that a short bunch length can still be achieved by adjusting the linac phase. It has been observed from simulation

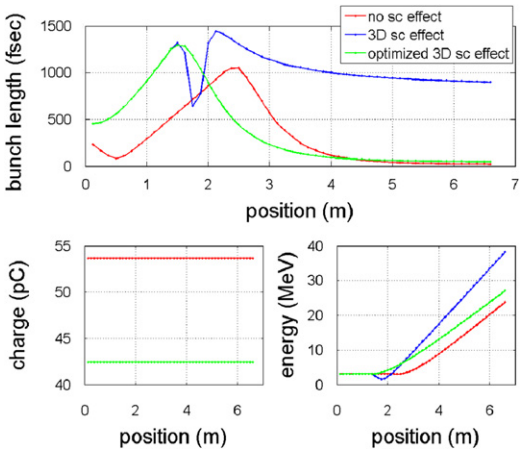

Fig. 6. Top: Evolution of the bunch length along the beamline after the alpha magnet, as simulated by GPT with the injection phase at the rf zero crossing when the space charge effect is turned off (red); the 3D space charge effect is turned on (blue); and the 3D space charge effect is turned on, but the injection phase is readjusted to minimize the bunch length (green). Lower left: Bunch charge as a function of the longitudinal position along the beamline. Lower right: Average beam energy as a function of the longitudinal position along the beamline. (For interpretation of the references to colour in this figure legend, the reader is referred to the web version of this article.)

Table 1
Designed parameters of the NSRRC inverse Compton scattering experiment.

Laser beam		Electron beam	
Wavelength	800 nm	Energy	27.08 MeV
Pulse energy	3.75 mJ	Charge	42.4 pC
Pulse length	100 fs	Bunch length	49 fs
Beam size	30 μm	Beam size	30 μm
X-ray pulse			
Photon energy		17.42 keV	
Pulse duration		49 fs	
Photon number		4.45×10^4 photons	
Peak photon flux		9.08×10^{17} photons/s	

results that there is a slight increase of electron loss on the collimator, as well as a beam energy gain, due to the space charge effect in the beam. With the space charge effect taken into account, the shortest bunch length of 49 fs can be found when the beam energy is 27 MeV and the electron bunch charge is 42.4 pC.

4. Conclusion

The design study of a driver linac to generate a GHz-repetition-rate ultra-short relativistic electron beam for a femtosecond head-on ICS X-ray source has been carried out. It has been found that 49-fs, 27-MeV relativistic electron pulses of 42 pC can be obtained by compressing the bunches with an alpha magnet and an rf linac operating at the injection phase near the zero crossing. We also found that velocity bunching in the booster linac also plays an important role in this bunch length compression scheme. It allows the operation of an ultra-short ICS X-ray source at a 0.7-Å wavelength, with a peak photon flux of 9.08×10^{17} photons/s. Table 1 provides a summary of the designed parameters of our head-on ICS experiment. Beam focusing to a few tens

micrometers at the interaction point and emittance evolution along the beamline require further investigation.

Acknowledgments

The authors would like to thank Professor Helmut Wiedemann and Professor Hiroyuki Hama for their continuous guidance and encouragement regarding the study of this subject. We also appreciate the assistance from Dr. Max Cornacchia and Dr. Michael Borland, especially on the subject of the usage of simulation tools.

References

[1] K.J. Gaffney, et al., Science 316 (2007) 1444.
[2] P. Kung, et al., Phys. Rev. Lett. 73 (1994) 967–970.
[3] S.K. Ride, et al., Phy. Rev. E 52 (1995) 5.
[4] S. Rimjaem, et al., Nucl. Instr. and Meth. A 533 (2004) 258–269.
[5] L. Serafini, A. Bacci, M. Ferrario, Proceedings of 2001 Particle Accelerator Conference, 2001, pp. 2242–2244.
[6] L. M. Young, LANL report LA-UR-96-1835, 2005.
[7] M. Borland, elegant: A Flexible SDDS-compliant Code for Accelerator Simulation, APS report LS-287, September 2000.
[8] S.B. van der Geer, M.J. de Loos, General Particle Tracer, User manual, version 2.82, 2008.